X-ray Photon Correlation Spectroscopy Applied to the Study of a Martensitic Transformation

L. Müller[a], M. Waldorf[a], C. Gutt[b], A. Madsen[c], G. Grübel[b], T.R. Finlayson[d] and U. Klemradt[a]

[a] *Physikalisches Institute II, RWTH Aachen University, Germany.*
[b] *Hasylab at DESY, Hamburg, Germany.*
[c] *European Synchrotron Research Facility, Grenoble, France.*
[d] *School of Physics, University of Melbourne, Victoria 3010, Australia.*

Some important features of the martensitic transformation and its application involving the shape memory phenomenon are reviewed, indicating a requirement to study dynamical aspects of the transformation. The basic principles of x-ray photon correlation spectroscopy are discussed and the technique has been applied for the first time to study the martensitic transformation in a $Au_{50.5}Cd_{49.5}$ single crystal. The results are best analysed using a two-time correlation function and indicate both slow and fast dynamics in the vicinity of the transformation temperature.

1. Introduction

The martensitic transformation can be broadly classified as a "lattice-distortive, shear-dominant, diffusionless, first-order, phase transition" [1]. The untransformed, or higher-temperature (higher-symmetry), parent phase is generally called austenite while the transformed, lower-temperature and lower-symmetry product phase is called martensite. The structural transition for most materials exhibiting such transformations is induced by a change in temperature, leading to characteristic temperatures, M_s (martensite start) and M_f (martensite finish) on cooling and A_s and A_f (austenite start and finish) for the reverse transformation on heating. Different material systems exhibiting martensitic transformations show different degrees of thermal hysteresis ranging from a couple of hundred to only a few degrees. The transformation can also be induced in some materials by the application of a stress (and thus strain) field or by an applied magnetic field (via a magnetostrictive-like coupling to the crystallographic strain).

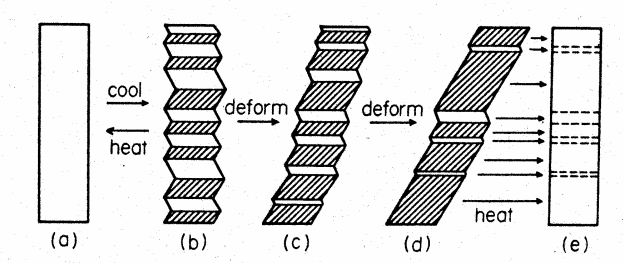

Fig. 1. Illustration of the mechanism for the shape memory effect (after Otsuka *et al.* [2])

For a martensitic transformation exhibiting relatively small thermal hysteresis (typically a few to 10s of degrees), the transformation strain is fully recoverable whether it be induced by temperature change or deformation, leading to the shape-memory effect (illustrated schematically in Fig. 1) which has given rise to various applications as actuators, transducers, couplings and fasteners [2] for some of the large number of materials exhibiting it. While Nitinol (a Ni-Ti alloy) is the material one finds most widely used in applications, other

examples, such as Au-Cd, one of the first shape-memory alloys discovered [3], have been model systems for scientific investigations. The overall external strain exhibited by a sample consists of both an atomic scale component arising from the crystallographic transformation of the material and a component at the mesoscopic scale, being a consequence of the development of twin variants in the microstructure. The underlying physics of such materials has been a topic of considerable discussion particularly in relation to: (i) the driving mechanism for the transformation; (ii) its nucleation; (iii) precursor effects in the parent phase; and (iv) the transformation dynamics and the precise microstructural scale controlling the dynamics [1]. In relation to (iii) several systems exhibit phonon softening in the parent phase with consequent anomalous temperature dependences being exhibited by physical properties [4].

Transformations amongst the various materials appear to be either athermal (implying that the amount of a sample transformed depends on temperature but is independent of time) or isothermal (i.e., the amount of the sample transformed on holding at constant temperature is a function of time). In recent years there has been a growing number of reports of time-dependent phenomena as summarized in Table 1, particularly for a sample held at a constant temperature with time, a few degrees above its M_s, (a phenomenon called incubation). Surprisingly, the list contains some materials which transform athermally below M_s. Some of these results were reviewed recently by Müller *et al.* [14].

Table 1. Incubation for various martensitic alloys

Alloy	M_s (K)	ΔT (K) (= $T - M_s$)	Incubation Time	Property Studied	Reference
$In_{77}Tl_{23}$	250	6.7	1-10 h	X-ray Diffraction	[5]
$Fe_{68.4}Ni_{31.6}$	177	7	1-50 m	Electrical Resistance	[6]
$Cu_{67.3}Al_{29.1}Ni_{3.6}$	220	5	1.7 m -2.8 h	Electrical Resistance	[7]
$Au_{50.5}Cd_{49.5}$	300.3	2.7	0.5-2.5 s	Electrical Resistance	[8]
Na	32	6	3 h	Electrical Resistance	[9]
$Au_{52.5}Cd_{47.5}$	312	4	3-21 h	Neutron Diffraction	[10]
$Ni_{63}Al_{37}$	282.2	0.6	1 s –2.7 h	Light Scattering	[11]
$Au_{51.75}Cd_{47.5}Cu_{0.75}$	260	1.4	1-4 h	X-ray Diffraction	[12]
$Au_{51.75}Cd_{47.5}Cu_{0.75}$	267-272	8	5 m -5 h	X-ray Diffraction	[13]

2. Au-Cd sample

$Au_{50.5}Cd_{49.5}$ is one such shape-memory material, which transforms from a β_2 (CsCl-type cubic) parent structure to a ζ_2' (trigonal) martensite with $M_s \approx 305$ K. In various studies [15,16,17], A_s and A_f have been found to increase following holding the sample in its martensite state while in one study [15], M_s was observed to decrease following constant temperature holding in its austenite state. The mechanism for the "martensite ageing effect" has also been widely discussed [18] and the most accepted concept is the "symmetry-conforming short range order" (SC-SRO) principle [19] based on an equilibrium distribution of point defects following the symmetry of the crystal. For the current experiments a single crystal piece with a polished (001) surface was available.

3. Experimental method

The initial motivation was to employ a technique which would provide quantitative data concerning microstructural fluctuations within the crystal. Traditionally, the dynamics of fluctuations in transparent systems, such as particle suspensions, have been measured by dynamic light scattering. If the experiment is performed using highly coherent laser light, the scattering pattern exhibits random interferences, or "speckles" and the dynamics of the particles in the suspension are directly related to the intensity fluctuations of the speckle pattern, in a technique called photon correlation spectroscopy. The dynamics of polymer suspensions and gels have been extensively studied by this technique [20].

With the advent of highly coherent and high-brilliance x-ray sources at synchrotrons, the spectroscopy has been extended to study microstructural fluctuations at the crystallographic scale, a technique known as x-ray photon correlation spectroscopy (XPCS). Examples in the literature include colloidal suspensions [21], polymer micelle liquids [22], the dynamics of anti-phase domains in an ordered $Co_{60}Ga_{40}$ alloy [23] and antiferromagnetic domain wall fluctuations in Cr [24]. In a shape memory alloy being cooled towards M_s a likely scenario for the transformation consists of the development of dynamical embryos of the martensite phase embedded in the austenite phase but interacting with one another and the austenite matrix via elastic forces. As the transition is approached the number of embryos increases dramatically, until below the transition, domains (martensite variants) develop as determined by the allowed twinning relationships for the new structure. Thermodynamically, such behaviour is analogous to that for a second-order phase transition for which one expects a critical slowing down of fluctuations in the vicinity of the transition temperature [25].

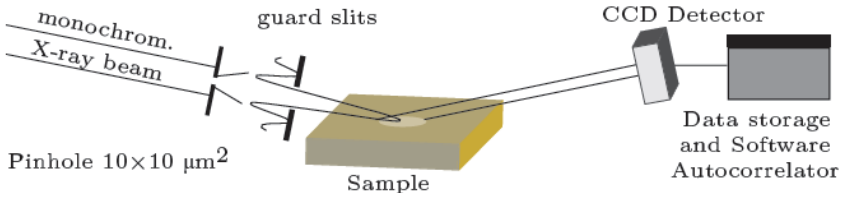

Fig. 2. Schematic setup for x-ray photon correlation spectroscopy measurements.

The schematic set-up for the measurements which were undertaken using 8 keV x-rays at the ESRF ID10A beamline, is illustrated in Fig. 2. The high-brilliance, longitudinally coherent x-ray beam was intercepted by a pinhole aperture, 10×10 μm^2, located about 50 cm in front of the sample to achieve transverse coherence. The additional guard slits suppress scattered radiation from the pinhole aperture. The crystal was contained in a specially designed cryofurnace which enabled the crystal temperature to be controlled with a stability of ± 3 mK and a resolution of 0.1 K for temperatures in the range 370 – 260 K. The temperature was decreased stepwise in 1 K increments from approximately 5 K above M_s and 0.1 K increments below 306 K through the transition. In addition, reference data were recorded at 360 K, 330 K and 270 K. In detecting the (001) Bragg reflection from the crystal, an area of its surface of about 10×45 μm^2 was illuminated. The Bragg reflection data were measured using a 650×401 pixel CCD detector with a pixel size of 22.5×22.5 μm^2. A time of 10 minutes was allowed for equilibration and then at each temperature 1,100 images were recorded, one every 1.4 s comprising a 0.2 s exposure followed by a 1.2 s data readout.

3. Results

Typical results for the summed intensities from all 1,100 exposures at each of three temperatures, 360 K (in the austenite phase), 305.5 K (in the vicinity of M_s) and 270 K (in the martensite phase) are illustrated in Fig. 3. The peak splitting expected at this lowest

temperature is clearly seen. Observable changes in the recorded images occurred at temperatures as high as M_s + 30 K, indicating the onset of microstructural changes in the crystal well above the transition temperature, consistent with precursive effects found in other shape memory alloys [26,27].

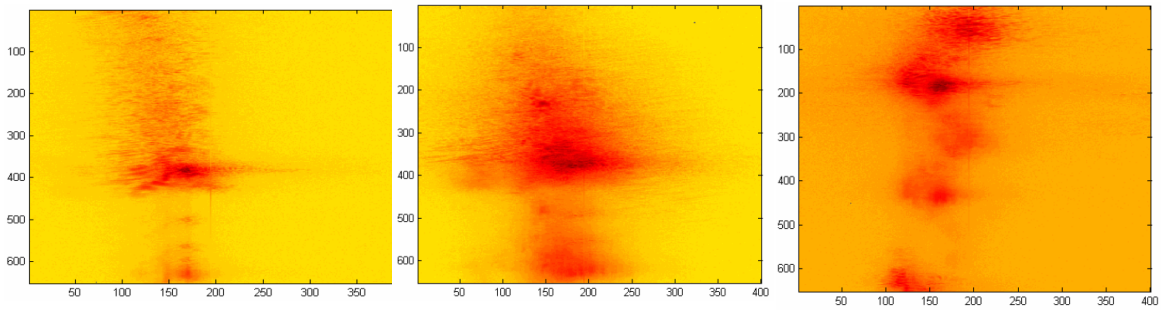

Fig. 3. Images of summed CCD exposures for the (001) Bragg reflection from the $Au_{50.5}Cd_{49.5}$ single crystal at 360 K, (left), 305.5 K (centre) and 270 K (right).

The data at each temperature were initially analysed by numerical integration over the CCD area in steps centred on the maximum intensity and equivalent to steps in q of 0.004 Å $^{-1}$. The time-averaged, one-time correlation function

$$g_2(q,\tau)=\frac{\langle I(t)\cdot I(t+\tau)\rangle_t}{\langle I(t)\rangle_{0\le t\le t_{run}-\tau}\cdot\langle I(t)\rangle_{\tau\le t\le t_{run}}} \tag{1}$$

$$=1+A|f_1(\tau)|^2 \tag{2}$$

where $$\langle I(t)\cdot I(t+\tau)\rangle=\frac{1}{T}\int_0^T dt\,.I(t)I(t+\tau) \qquad T >> T_C \tag{3}$$

with T_C being the coherence time for intensity fluctuations. A denotes the speckle contrast. $f_1(\tau)$ is the intermediate scattering function which, in the case of equilibrium dynamics can be expressed as

$$f_1(\tau)=\exp\left(-\left(\frac{\tau}{\tau_0}\right)^{\beta}\right) \tag{4}$$

with the characteristic time scale, τ_0, and a stretching exponent, β. The results for τ_0 and β as functions of temperature in the vicinity of M_s, are shown in Fig. 4. Surprisingly, the result for τ_0 shows a decreasing time scale in the vicinity of the transition, contrary to the "critical slowing down" expected for such a phase transition, indicating that non-equilibrium behaviour may be occurring in the system.

For this reason data analysis was undertaken using a two-time correlation function [28]

$$C_2(q,t_1,t_2)=\frac{I(t_1)\cdot I(t_2)}{\langle I(t_1)\rangle_t\cdot\langle I(t_2)\rangle_t} \tag{5}$$

This analysis was carried out using the 305.3 K data set and for an area in the Bragg reflection image corresponding to a Δq of 0.005 Å^{-1} around the position of maximum intensity. The result is illustrated in Fig. 5. The diverging contours and the sharp cuts in the correlation function, shown by the partitions in the figure, are indications of non-equilibrium dynamics.

To study the sharp cuts in the correlation function, images were averaged over ten frames of raw data and the differences between successive averages plotted as a function of absolute time (Fig. 6). The result shows that the sharp cuts in the two-time correlation function are the result of a rapid process, the time scale for which could not have been resolved in the present experiment on account of the frame rate limitation. The time scales for the slow non-equilibrium dynamics were extracted by calculating the non-time-averaged, one-

time correlation function at each absolute time for the recorded data. This can be done via an integration along a -45-degree line extending from the bisectrix of the two-time correlation function result (Fig. 5). Each of these correlation functions can then be analysed using the stretched exponential function (Eq. 4). The results for τ_0 and β versus absolute time, t_{abs}, which is really the ageing time for the alloy at the particular temperature (305.3 K), are shown in Fig. 7. τ_0 vs t_{abs} shows a strong deceleration of the dynamics with ageing time while the time dependence of β shows significant dips at times similar to those of the peaks in Fig. 6.

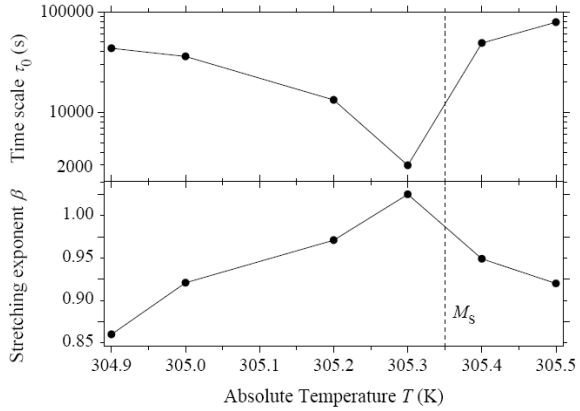

Fig. 4. Results for the characteristic time, τ_0, and the stretching exponent, β, at various temperatures near M_s, determined from data fits using the one-time correlation function.

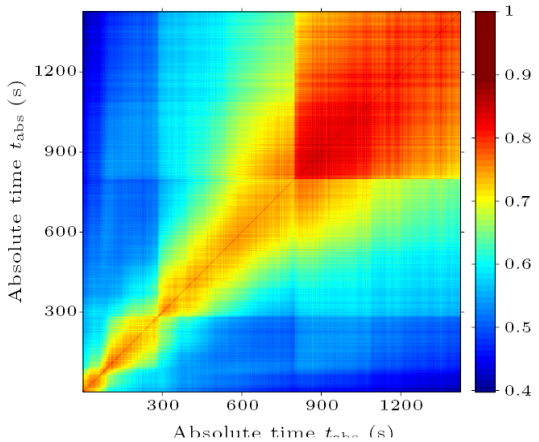

Fig. 5. Two-time correlation function for data recorded at 305.3 K, calculated for a circular region around the maximum of the Bragg reflection.

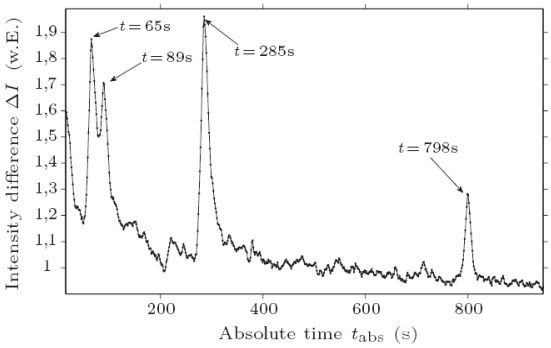

Fig. 6. Sequential intensity differences for averages over 20 exposures, for the data analysed in Fig. 5, as a function of absolute time.

4. Discussion

The two non-equilibrium processes, the one fast (or avalanche-like) and the other slow, can be understood in relation to microstructural changes which have been suggested in the literature. Rapid, non-equilibrium dynamics occur during the incubation time when discontinuous martensite interface motion occurs as the result of depinning from defect sites in the crystal. Such effects are known to be responsible for strong acoustic emission signals in shape memory alloys [29].

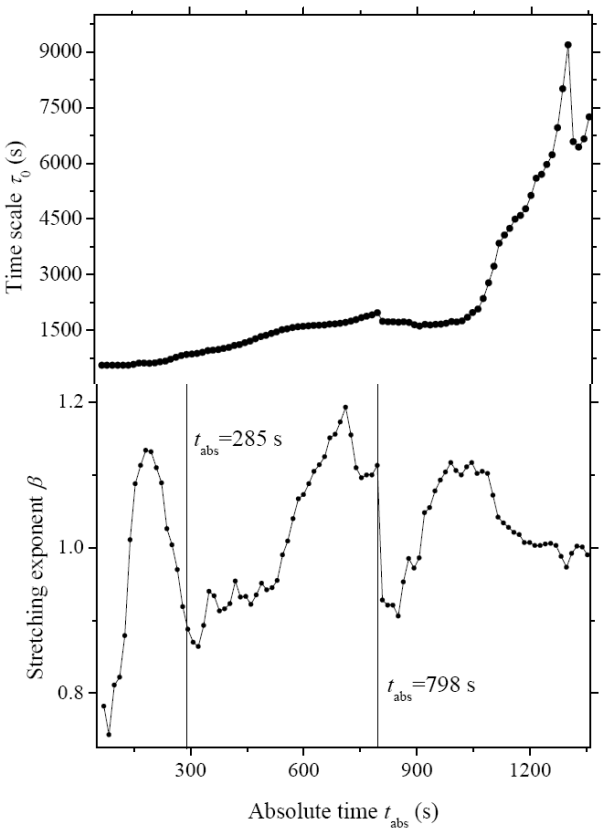

Fig. 7. Characteristic time, τ_0, and stretching exponent, β, extracted from the two-time correlation function at 305.3 K

Slow, non-equilibrium dynamics are consistent with the martensite ageing process which has been best described microstructurally on the SC-SRO model [19] involving a diffusive rearrangement of lattice defects, consistent with the local reduction in symmetry to that of the transformed phase.

5. Conclusions

In this project x-ray photon correlation spectroscopy has been employed to study the dynamics of the martensitic transformation in a $Au_{50.5}Cd_{49.5}$ single crystal. The critical slowing down expected for such a transformation was not observed. Rather an analysis of the data using a two-time correlation function indicated non-equilibrium dynamics exhibiting two time scales, the one fast, consistent with discontinuous, avalanche-like, microstructural changes and the other slow, consistent with a diffusive rearrangement of lattice defects. The latter process is consistent with the symmetry-conforming-short-range-order model.

Acknowledgements

We acknowledge support for access to ESRF beamline ID10A and the assistance of the beamline staff during the experiments. TRF acknowledges the support of a Renewal of Fellowship Grant from the Alexander von Humboldt Foundation, during the early stages of this research collaboration.

References

[1] Olsen G B and Owen W S (eds) 1992 *Martensite* (ASM International)
[2] Otsuka K and Wayman C M (eds) 1998 *Shape Memory Materials* (Cambridge University Press) Chapters 10, 11 and 12
[3] Chang L C and Read T A 1951 *Trans A.I.M.E.* **189** 47
[4] Finlayson T R 1988 *Met. Trans. A* **19** 185
[5] Abe H, Ishibashi M, Oshima K, *et al.* 1994 *Phys. Rev. B* **50** 9020
[6] Kakeshita T, Fukuda T and Saburi T 1996 *Scripta Mater.* **34** 147
[7] Kakeshita T, Takeguchi, Fukuda T, *et al.* 1996 *Met. Trans. J.I.M.* **37** 299
[8] Kozuma M, Murakami Y, Kawano T *et al.* 1997 *Scripta Mater.* **36** 253
[9] Abe H and Oshima K 1998 *J. Phys. Soc. Jpn.* **67** 2952
[10] Ohba T, Komachi K, Watanabe K, *et al.* 1999 *Mater. Sci. & Eng. A* **273-275** 554
[11] Aspelmeyer M, Klemradt U, Wood L T, *et al.* 1999 *phys. stat. sol. (a)* **174** R9
[12] Abe H, Matsuo Y and Oshima K 1999 *J. Phys. Soc. Jpn.* **68** 2648
[13] Saitoh H, Fujimoto M, Abe H, *et al.* 2001 *Mater. Sci. & Eng. A* **312** 20
[14] Müller L, Klemradt U and Finlayson T R 2006 *Mater. Sci. & Eng. A* **438-440** 122
[15] Murakami Y, Morito S, Nakajima Y, *et al.* 1994 *Mater. Lett.* **21** 275
[16] Kuroiwa Y, Finlayson T R and Smith T F 1999 *J. Mater. Sci. Lett.* **18** 2045
[17] Finlayson T R, Kelly G L, Ersez T, *et al.* 2000 *Mater. Sci. Forum* **327-3** 457
[18] Otsuka K and Ren X 2004 *Scripta Mater.* **50** 207
[19] Ren X and Otsuka K 1997 *Nature* **389** 579
[20] Patterson G D 1983 in *Light Scattering from Polymers* (Springer-Verlag) pp125-159
[21] Thurn-Albrecht T, Steffen W, Patkowski A, *et al.* 1996 *Phys. Rev. Lett.* **77** 5437
[22] Mochrie S G C, Mayes A M, Sandy A R, *et al.* 1997 *Phys. Rev. Lett.* **78** 1275
[23] Stadler L-M, Sepiol B, Kantelhardt J W, *et al.* 2004 *Phys. Rev. B* **69** 224301
[24] Shpyrko O G, Isaacs E D, Logan J M, *et al.* 2007 *Nature* **447** 68
[25] Cowley R A 1980 *Adv. in Phys.* **29** 1
[26] Fromm M, Klenradt U, Landmesser G, *et al.* 1999 *Mater. Sci. & Eng. A* **273-275** 291
[27] Shapiro S M, Yang B X, Noda Y, *et al.* 1991 *Phys. Rev. B* **44** 9301
[28] Malik A, Sandy A R, Lurio L B, *et al.* 1998 *Phys. Rev. Lett.* **81** 5832
[29] Planes A, Perez-Reche F-J, Vives E, *et al.* 2004 *Scripta Mater.* **50** 181